

# Nonsequential Double Recombination in Intense Laser Fields

P. Koval, F. Wilken, D. Bauer,\* and C.H. Keitel

Max-Planck-Institut für Kernphysik, Postfach 103980, 69029 Heidelberg, Germany

(Dated: February 9, 2020)

A second plateau in the harmonic spectra of a laser-driven two-electron model atom is observed. It is shown that the harmonics well beyond the usual cut-off are due to the simultaneous recombination of the two electrons, which were emitted during different, previous half-cycles. The new cut-off is explained in terms of classical trajectories. Classical predictions and the time-frequency analysis of the *ab initio* quantum results are in excellent agreement. The mechanism corresponds to the inverse single photon double ionization process in the presence of a (low frequency) laser field. The rather low efficiency of the process is shown to be substantially enhanced by controlling the electron emission times using attosecond xuv pulses.

PACS numbers: 42.65.Ky, 32.80.Rm, 34.80.Lx, 32.80.Wr

High-order harmonic generation (HOHG) is one of the fundamental processes that occur when intense laser pulses interact with atoms or molecules (see, e.g., Refs. [1, 2] for recent reviews). In the case of a linearly polarized incoming laser field, odd multiples of the laser frequency are emitted with a relatively high and almost constant efficiency ( $\simeq 10^{-6}$ ) up to the celebrated  $I_p + 3.17 U_p$  cut-off [3], where  $I_p$  is the ionization potential and  $U_p$  is the ponderomotive energy (i.e., the time-averaged quiver energy of a free electron in the laser field). In such a way, coherent short-wavelength radiation down to the “water window” could be generated using “table-top” equipment [4, 5]. HOHG is also the key to the production of attosecond laser pulses [1, 2] that offer the possibility to study fast atomic processes directly in the time domain [6].

HOHG up to the  $I_p + 3.17 U_p$  cut-off is, in a very good approximation, a single active electron-effect, meaning that at a given laser intensity only a single electron, namely the one that is next in the row for sequential ionization, contributes to the harmonic generation. Various aspects of two- and many-electron effects on HOHG were studied in Refs. [7, 8, 9, 10, 11, 12]. However, to the best of our knowledge nonsequential double recombination (NSDR) and the associated second plateau has not been revealed so far.

The known cut-off at  $I_p + 3.17 U_p$  can be explained within the so-called “simple man’s theory” (see, e.g., the review Ref. [14] and references therein): an electron is released with vanishing initial velocity at the emission time  $t_e$  due to ionization by a laser field with a vector potential  $\mathbf{A}(t)$  and an electric field  $\mathbf{E}(t) = -\partial_t \mathbf{A}(t)$ . Thereafter, the electron moves freely in the laser field without being affected anymore by the binding potential  $V(\mathbf{r})$ , i.e., its momentum and position at time  $t > t_e$  are given by  $\mathbf{p}(t) = \mathbf{A}(t) - \mathbf{A}(t_e)$  and  $\mathbf{r}(t) = \boldsymbol{\alpha}(t) - \boldsymbol{\alpha}(t_e) - \mathbf{A}(t_e)(t - t_e)$ , respectively, where  $\boldsymbol{\alpha}(t) = \int^t dt' \mathbf{A}(t')$  is the excursion of a free electron in the field (atomic units  $\hbar, m, |e|, 4\pi\epsilon_0 = 1$  are used unless noted otherwise). In order for a harmonic photon being emitted, the electron has to revisit the ion at some time  $t_r > t_e$ , that is,  $\mathbf{r}(t_r) \stackrel{!}{=} 0$ , since only then

its overlap with the ground state—and thus the recombination probability—is appreciable. The energy of the emitted harmonic photon is given by  $\Omega = \mathbf{p}^2(t_r)/2 + I_p$ . Searching the pairs  $(t_e, t_r)$  for which  $\mathbf{r}(t_r) = 0$  and  $\mathbf{p}^2(t_r)/2$  is maximum, leads in the case of a constant-amplitude, linearly polarized laser field in dipole approximation, e.g.,  $\mathbf{A}(t) = \hat{A} \mathbf{e}_z \sin \omega t$ , to  $\max(\mathbf{p}^2(t_r)/2) = 3.17 U_p$  where  $U_p = \hat{A}^2/4$ .

Let us now consider a two-electron atom or ion where the two electrons are freed by sequential ionization. The possible kinetic return energies  $E_r = \mathbf{p}^2(t_r)/2$  are shown in Fig. 1. Each of the two electrons has a maximum return energy  $3.17 U_p$ . If both electrons moved along the same trajectory in the continuum and recombined together, emitting a *single* photon, one would expect a HOHG cut-off at  $2 \cdot 3.17 U_p + I_p^{(1)} + I_p^{(2)}$  with  $I_p^{(i)}$  the ionization potential for the  $i$ th electron. However, electron repulsion renders this process extremely unlikely since the two electrons would have to “sit on top of each other” for about half a laser cycle (which is even less likely than “collective tunneling” [13]). Instead, if the electrons are emitted at certain times during subsequent or next but one half cycles, there are trajectories that do not cross before the recombination event, so that their mutual repulsion plays only a minor role (and is compensated by the attraction of the ionic potential). Such trajectories are shown in Fig. 1b. If, with respect to the first electron, the second electron is emitted during the subsequent half cycle, the sum of return energies around its maximum value is shown in Fig. 1a (indicated by “2 + 1”). For the constant-amplitude pulse one finds  $4.70 U_p$ . If, however, the delay between the emission of first and second electron is greater than half a cycle the sum of the return energies can be even higher, as clearly visible from the values labelled by “3 + 1” in Fig. 1a. The HOHG cut-off for NSDR is then expected at

$$\max(\Omega_{\text{NSDR}}) = 5.55 U_p + I_p^{(1)} + I_p^{(2)}.$$

In the following, we will show that this cut-off can be clearly identified in *ab initio* solutions of the two-electron,

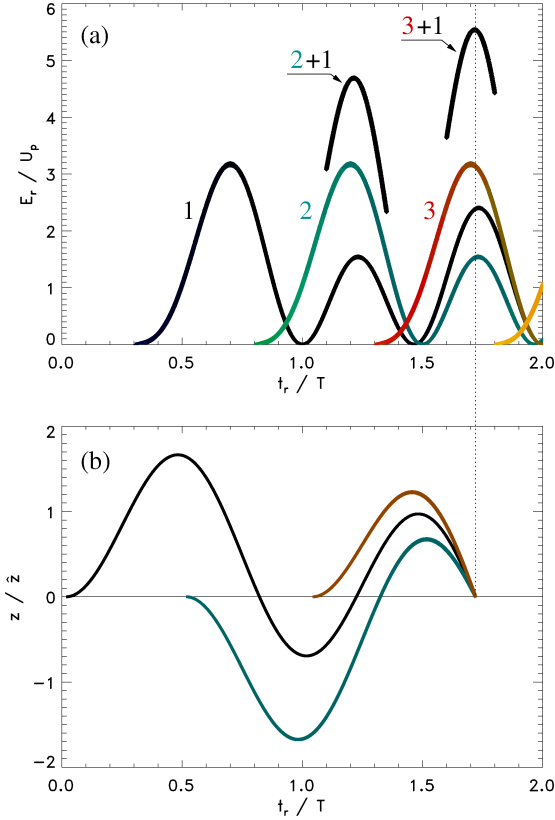


FIG. 1: (color online). Return energies  $E_r$  in units of  $U_p$  (a) and the excursion  $z$  in polarization direction in units of  $\hat{z} = \hat{A}/\omega$  vs the return time  $t_r$  in laser cycles for a laser field  $\mathbf{A}(t) = \hat{A}e_z \sin \omega t$ . Electrons emitted during the first half cycle (1, black), the second (2, cyan), the third (3, red) etc. reach their maximum return energy  $3.17 U_p$  during the subsequent half cycle. At later returns only lower values are achieved. However, if these energies are added to those of a second electron returning at the same time (but ionized later than the first electron), the values indicated by “2 + 1” and “3 + 1” are obtained (the sum “3+2” equals “2+1” in height and is omitted in the plot). The three classical trajectories of electrons, all returning at  $t_r/T = 1.72$  (vertical dotted line), are plotted in (b).

time-dependent Schrödinger equation.

We employ a widely used one-dimensional (1D) model He-atom [15] to study NSDR on an *ab initio* time-dependent Schrödinger equation (TDSE)-level. The Hamiltonian in dipole approximation reads

$$\hat{H}(t) = \sum_{i=1}^2 \left( \frac{[p_{ci} + A(t)]^2}{2} + V(x_i) \right) + W(x_1 - x_2),$$

with  $V(x_i) = -Z(x_i^2 + \epsilon_{ei})^{-1/2}$ ,  $W(x_1 - x_2) = [(x_1 - x_2)^2 + \epsilon_{ee}]^{-1/2}$ ,  $Z = 2$ , and  $p_{ci}$  the canonical momenta of the two electrons, i.e.,  $\dot{x}_i = p_{ci} + A(t)$ . The soft-core parameters  $\epsilon_{ei}$ ,  $\epsilon_{ee}$  can be tuned in such a way that the model ionization potentials  $I_p^{(i)}$  equal the real ones of the

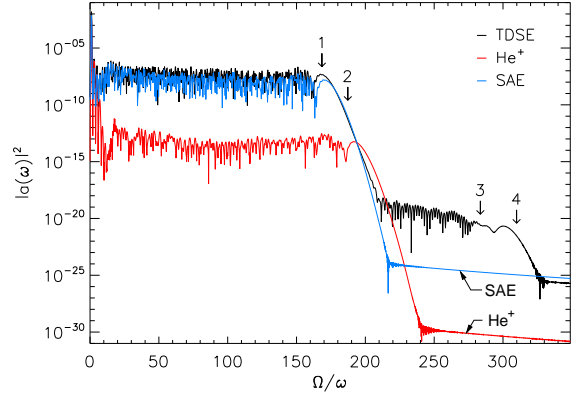


FIG. 2: (color online). HOHG spectra for a  $n = 6$ -cycle laser pulse with  $\omega = 0.0584$  and  $\hat{A} = 3.417$  ( $I = 1.4 \cdot 10^{15} \text{ Wcm}^{-2}$ ). The spectrum for the He-model with both electrons active (drawn black) shows a second plateau. The corresponding single active electron (SAE)-result and the spectrum obtained from the  $\text{He}^+$ -ion are also included. The arrows indicate the expected cut-off positions (see text).

3D He atom. The actual values were  $\epsilon_{ei} = 0.5$  (which yields the correct  $I_p^{(2)} = 2.0$  for  $\text{He}^+$ ) and  $\epsilon_{ee} = 0.329$  (so that  $I_p^{(1)} = 0.904$ ) [16]. The TDSE  $i\partial_t \Psi(x_1, x_2, t) = \hat{H}(t)\Psi(x_1, x_2, t)$  was solved on a  $x_1, x_2$ -grid ( $\Delta x = 0.2$ ) using a split-operator Crank-Nicolson approach ( $\Delta t = 0.075$ ), starting at  $t = 0$  with the spatially symmetric spin-singlet ground state wave function. The  $n$ -cycle laser pulse was of the form  $A(t) = \hat{A} \sin^2(\omega t/2n) \sin \omega t$  for  $0 \leq t \leq nT$  and zero otherwise (with  $T = 2\pi/\omega$ ). The harmonic spectra are calculated from the modulus-square of the Fourier-transformed expectation value of the acceleration [17]  $a(t) = \sum_{i=1}^2 \langle \ddot{x}_i(t) \rangle = \sum_{i=1}^2 \langle \dot{p}_{ci}(t) + \dot{A}(t) \rangle = \int dx n(x, t) [-\partial V/\partial x - E(t)]$  where  $n(x, t)$  is the density (normalized to the number of electrons),  $E(t) = -\hat{A}(t)$ , and use of Ehrenfest’s Theorem and the fact that  $\partial W/\partial x_1 = -\partial W/\partial x_2$  was made.

Results for HOHG spectra obtained from the He model atom exposed to a  $n = 6$ -cycle laser pulse with  $\omega = 0.0584$  and  $\hat{A} = 3.417$  ( $I = 1.4 \cdot 10^{15} \text{ Wcm}^{-2}$ ) are shown in Fig. 2. Besides the result for the fully correlated system with both electrons active, the corresponding spectra for a frozen, inner electron (labelled “SAE”, drawn blue) and  $\text{He}^+$  (drawn red) are shown. For the single active electron (SAE)-calculation, a frozen Hartree-Fock potential (leading to the proper ionization potential for the outer electron  $I_p^{(1)} = 0.904$ ) was used. Not surprisingly, the SAE spectrum agrees well with the two active electron (TAE)-result throughout the “usual” plateau (whose cut-off  $3.17 U_p + I_p^{(1)}$  [18] is indicated by arrow 1) because at the chosen laser intensity it is the outer electron that contributes most to HOHG. As expected, the plateau of the  $\text{He}^+$ -spectrum is several orders of magnitude lower

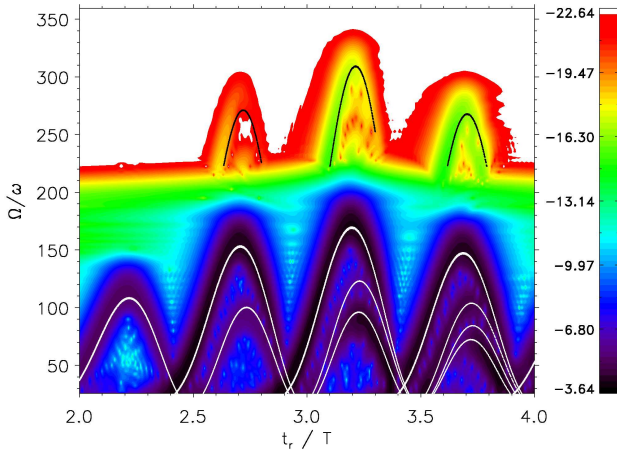


FIG. 3: Time-frequency analysis of the HOHG spectrum in Fig. 2, showing the color-coded contour plot of  $\log_{10} |a(\omega, t)|^2$ . The relevant classical solutions for the 6-cycle  $\sin^2$ -pulse (corresponding to those shown in Fig. 1a for the constant-amplitude pulse) are superimposed. The possible classical recombination energies of a single electron  $\Omega = E_r + I_p^{(1)}$  are drawn white. The sums of the two highest classical return energies  $E_{r1}, E_{r2}$  plus the two ionization potentials,  $\Omega = \sum_i [E_{ri} + I_p^{(i)}]$ , are superimposed in black for the recombination times  $t_r$  of interest.

in efficiency. The  $\text{He}^+$  HOHG-cut-off is expected at  $3.17 U_p + I_p^{(2)}$  (indicated by arrow 2). Neither the SAE- nor the  $\text{He}^+$ -spectrum show a second plateau. The TAE-result, however, confirms our above considerations. Arrows 3 and 4 indicate the positions  $4.70 U_p + I_p^{(1)} + I_p^{(2)}$  and  $5.55 U_p + I_p^{(1)} + I_p^{(2)}$ , respectively [18].

Switching-off electron-electron correlation in the two-electron TDSE-code is equivalent to the simulation of two independent  $\text{He}^+$ -ions. For the latter, NSDR is impossible, showing that at the time of recombination, electron correlation is clearly required for NSDR to happen since otherwise the two electrons cannot emit their total energy in a *single* photon. This is well known for the inverse process, i.e., single photon double ionization.

It is interesting to see that around arrow 3 in Fig. 2 a qualitative change occurs: for lower harmonic frequencies the spectrum displays a rich interference structure because many “quantum trajectories” [14] contribute. The situation changes for the harmonic orders where only the classical solutions with  $t_r/T \in [3, 3.5]$  survive. There are only two such solutions (and finally, at the cut-off, only one), resulting in a much less jagged spectrum between arrows 3 and 4.

The classical trajectories directly emerge in the TDSE quantum results if a time-frequency analysis is performed. To that end a window is applied to the spectrum, selecting a certain frequency interval. The result is Fourier-transformed back, leading to a complex quantity  $a(\omega, t)$  containing information about when the

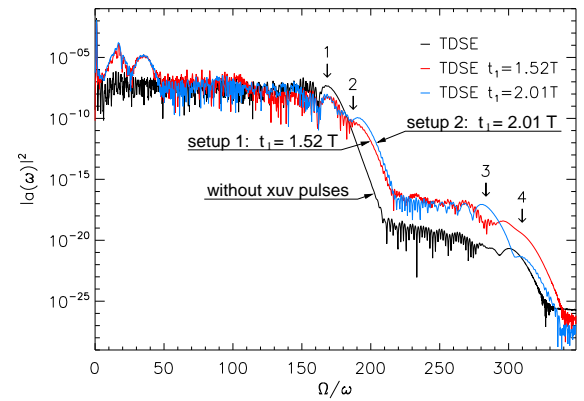


FIG. 4: (color online). Enhancement of NSDR by properly tailored xuv attosecond pulses  $A_i(t) = \hat{A}_i \exp[-\Gamma(t - t_i)^2] \sin[\omega_i(t - t_i)]$ ,  $i = 1, 2$ . The parameters were  $\omega_i = I_p^{(i)}$ ,  $\Gamma = 0.04$ ,  $t_2 = 2.54T$ ,  $A_2 = \omega_1 A_1 / \omega_2$ ,  $A_1 = 0.35$ . Results for two different values of  $t_1$  are shown, as indicated in the plot. Parameters for the infrared pulse as in Fig. 2.

selected harmonics are emitted. The structures in the time- and frequency-resolved radiated power  $|a(\omega, t)|^2$  reveal the relevant classical “simple man’s” solutions. The time-frequency analysis of the TAE-spectrum of Fig. 2 is shown in Fig. 3. The relevant classical “simple man’s” solutions are superimposed (analogous to Fig. 1). The recombination energies  $E_r + I_p^{(1)}$  of individual electrons are drawn white. In the frequency intervals of interest, the sum of the two classical highest return energies (plus the ionization potentials) are superimposed in black. The excellent agreement between “simple man’s” and *ab initio* quantum results shows that NSDR is indeed the mechanism behind the second plateau.

The remainder of this Letter is devoted to the control of the NSDR process with the goal to enhance its efficiency. Using the classical analysis above, the two relevant emission times contributing to NSDR at a given energy are readily calculated. In the case of the 6-cycle  $\sin^2$ -pulse one finds for, e.g., the NSDR cut-off energy, that the first electron should be emitted at  $t_1 = 1.52T$  and the second at  $t_2 = 2.54T$ . They then have the highest probability to both recombine at  $t_r = 3.2T$  with the highest possible joint return energy  $5.55 U_p$  (see Fig. 3). In the following we call this scenario “setup 1”. Instead, if  $t_1 = 2.01T$  is chosen the return energy  $4.70 U_p$  is favored (“setup 2”). The ionization probability at the desired times  $t_i$ ,  $i = 1, 2$  may be enhanced by applying xuv attosecond pulses centered around these times. In order to avoid any excess energy immediately after ionization  $\omega_i = I_p^{(i)}$  was chosen for the two xuv frequencies  $\omega_i$ . Hence, assuming a vanishing initial velocity in the “simple man’s” analysis is still appropriate, and the trajectories themselves do not—but only their weights—

change. For fixing the ionization times very precisely, the xuv pulses should be as short as possible. However, in actual calculations one has to find a compromise: if the duration of the xuv pulses is chosen too short, the wings of their Fourier-transform [which enters the calculation of  $a(\omega)$ ] may mask the NSDR-plateau [19].

Figure 4 shows the HOHG spectra obtained for setups 1 and 2. The simulation parameters are given in the caption. The comparison with the result of Fig. 2 (included in black) shows that the “usual” plateau is mainly modified around  $\omega_1/\omega = 15.5$ ,  $\omega_2/\omega = 34.2$ , and in the cut-off region. In the latter, the  $\text{He}^+$ -cut-off (arrow 2) is much more pronounced than without xuv pulses. However, the average level of the first plateau is not affected by the xuv pulses (see, e.g., the harmonics around  $\Omega/\omega \simeq 80$ ). Instead, the second plateau due to NSDR is enhanced by a factor  $\simeq 10^3$  for both setup 1 and 2, showing that the control schemes devised above work. Due to the width of the xuv pulses the NSDR plateau is amplified in a broad energy interval. However, it is clearly seen that setup 1 enhances the NSDR plateau up to the cut-off (arrow 4) while setup 2 is restricted to lower photon energies, as it is expected from the considerations above.

In conclusion, the existence of nonsequential double recombination in intense laser fields was revealed. In this process, two electrons are freed by the laser, move in the continuum, and are driven back to the ion by the laser, where they recombine together upon emission of their joint energy plus their ionization potentials as a *single* photon. Nonsequential double recombination may thus be viewed as the inverse process of single photon double ionization. Clearly, in either direction the process requires electron correlation. Nonsequential double recombination manifests itself in a second plateau in high-order harmonic generation spectra. This was demonstrated by solving the time-dependent Schrödinger equation of a two-electron model atom numerically. The main features of the harmonic spectra, including the position of the new cut-off, were explained in terms of classical trajectories. Moreover, it was shown how the rather low efficiency of the process may be enhanced by aiding the desired ionization times with the help of xuv attosecond pulses. We did not aim at exhausting the optimum enhancement. It is well possible that more sophisticated choices of the xuv pulses’ parameters exist that increase the nonsequential double recombination-efficiency further. Finally, it should be noted that, instead of simultaneous recombination, the two returning electrons may undergo elastic or inelastic  $(2e, ne)$ -scattering processes such as, e.g., nonsequential ionization involving  $2 + n$  electrons or higher-order above-threshold ionization.

This work was supported by the Deutsche Forschungsgemeinschaft.

---

\* Corresponding author’s e-mail: dbauer@mpi-hd.mpg.de

- [1] P. Agostini and L.F. DiMauro, *Rep. Prog. Phys.* **67**, 813 (2004).
- [2] A. Scrinzi, M.Yu. Ivanov, R. Kienberger, and D.M. Villeneuve, *J. Phys. B: At. Mol. Opt. Phys.* **39**, R1 (2006).
- [3] M. Lewenstein, Ph. Balcou, M.Yu. Ivanov, A. L’Huillier, and P.B. Corkum, *Phys. Rev. A* **49**, 2117 (1994).
- [4] Z. Chang, A. Rundquist, H. Wang, M.M. Murnane, and H.C. Kapteyn, *Phys. Rev. Lett.* **79**, 2967 (1997).
- [5] M. Schnürer, Ch. Spielmann, P. Wobrauschek, C. Streli, N.H. Burnett, C. Kan, K. Ferencz, R. Koppitsch, Z. Cheng, T. Brabec, and F. Krausz, *Phys. Rev. Lett.* **80**, 3236 (1998).
- [6] M. Drescher, M. Hentschel, R. Kienberger, M. Uiberacker, V. Yakovlev, A. Scrinzi, Th. Westerwalbesloh, U. Kleineberg, U. Heinzmann, and F. Krausz, *Nature* **419**, 803 (2002).
- [7] D.G. Lappas, A. Sanpera, J.B. Watson, K. Burnett, P.L. Knight, *J. Phys. B: At. Mol. Opt. Phys.* **29**, L619 (1996).
- [8] Xiao-Min Tong and Shih-I Chu, *Phys. Rev. A* **64**, 013417 (2001).
- [9] J. Prager, S.X. Hu, and C.H. Keitel, *Phys. Rev. A* **64**, 045402 (2001).
- [10] A.D. Bandrauk and HuiZhong Lu, *J. Phys. B: At. Mol. Opt. Phys.* **38**, 2529 (2005).
- [11] J. Zanghellini, Ch. Jungreuthmayer, and T. Brabec, *J. Phys. B: At. Mol. Opt. Phys.* **39**, 709 (2006).
- [12] R. Santra and A. Gordon, *Phys. Rev. Lett.* **96**, 073906 (2006); A. Gordon, F.X. Kärtner, N. Rohringer, and R. Santra, *ibid.* **96**, 223902 (2006).
- [13] U. Eichmann, M. Dörr, H. Maeda, W. Becker, and W. Sandner, *Phys. Rev. Lett.* **84**, 3550 (2000).
- [14] D.B. Milošević, G.G. Paulus, D. Bauer, and W. Becker, *J. Phys. B: At. Mol. Opt. Phys.* **39**, R203 (2006).
- [15] See, e.g., R. Grobe and J.H. Eberly, *Phys. Rev. Lett.* **68**, 2905 (1992); S.L. Haan, R. Grobe, and J.H. Eberly, *Phys. Rev. A* **50**, 378 (1994); D. Bauer, *Phys. Rev. A* **56**, 3028 (1997); D.G. Lappas and R. van Leeuwen, *J. Phys. B: At. Mol. Opt. Phys.* **31**, L249 (1998); M. Lein, E.K.U. Gross, and V. Engel, *Phys. Rev. Lett.* **85**, 4707 (2000); L. Roso, L. Plaja, P. Moreno, E.C. Jarque, J.R. Vázquez de Aldana, J. San Román, and C. Ruiz, *Laser Phys.* **15**, 1393 (2005).
- [16] One could also set  $\epsilon_{ee} = \epsilon_{ei}$  and use  $Z$  as the other free parameter. The results presented in this Letter are insensitive to such details of the model.
- [17] K. Burnett, V.C. Reed, J. Cooper, and P.L. Knight, *Phys. Rev. A* **45**, 3347 (1992); J.L. Krause, K.J. Schafer, and K.C. Kulander, *Phys. Rev. A* **45**, 4998 (1992).
- [18] Note that in few-cycle pulses the actual vector potential  $A(t)$  may never reach  $\hat{A}$ . As a consequence, the  $U_p$  to be used in the cut-off laws has to be adapted.
- [19] Gaussian shapes were used for the attosecond pulses. For a given “full width half maximum” (FWHM) in time, the Fourier-transformed Gaussian is narrower in frequency than is the  $\sin^2$ -pulse, reducing the “background” of the calculated HOHG spectra significantly.